Journal of Arid Environments 168 (2019) 17–25

Contents lists available at ScienceDirect

Journal of Arid Environments

journal homepage: www.elsevier.com/locate/jaridenv

Ephemeral sand river flow detection using satellite optical remote sensing

David Walker[a,*], Magdalena Smigaj[a], Nebo Jovanovic[b]

[a] School of Engineering, Newcastle University, Newcastle Upon Tyne, United Kingdom
[b] Natural Resource and Environment, Council for Scientific and Industrial Research (CSIR), Stellenbosch, South Africa

ARTICLE INFO

Keywords:
Alluvial aquifer recharge
Flow detection
NDWI
Sentinel-2
Sand river
South Africa

ABSTRACT

Ephemeral sand rivers are common throughout the world's dryland regions, often providing a water source where alternatives are unavailable. Alluvial aquifer recharge results from rare surface water flows. Assessment of surface flow frequency using traditional methods (rain or flow gauges) requires a high-density monitoring network, which is rarely available. This study aimed to determine if satellite optical imagery could detect infrequent surface flows to estimate recharge frequency. Well-used sensors (Landsat and MODiS) have insufficiently high spatio-temporal resolution to detect often short-lived flows in narrow sand rivers characteristic of drylands. Therefore, Sentinel-2 offering 10 m spatial resolution was used for the Shingwidzi River, Limpopo, South Africa. Based on an increase of Normalised Difference Water Index relative to the dry season reference value, detection of surface flows proved feasible with overall accuracy of 91.2% calculated against flow gauge records. The methodology was subsequently tested in the ungauged Molototsi River where flows were monitored by local observers with overall accuracy of 100%. High spatial and temporal resolution allowed for successful detection of surface water, even when flow had receded substantially and when the rivers were partially obstructed by clouds. The presented methodology can supplement monitoring networks where sparse rainfall or flow records exist.

1. Introduction

The world's dryland regions are characterised by low and variable rainfall, which, when combined with negligible groundwater contribution, cause rivers to remain dry with very occasional surface water flow. Where the underlying geology is of low permeability, such as Africa's crystalline basement, the sediments deposited by these “sand rivers” can form useful aquifers. Unfavourable climate and geology in these regions often leads to few other accessible water resources. Sand river water table depth is typically less than a few metres and recharge via surface flow is infrequent but regular. Hence, long-term groundwater depletion is not expected and sand rivers are considered a renewable resource (Owen, 1989).

Drylands incorporate hyper-arid, arid, semi-arid and dry sub-humid areas, which comprise 41.3% of the Earth's surface and are home to 2.1 billion people (UN, 2017). Hence, water resources contained within these alluvial aquifers provide for millions of people and have been utilised for millennia (Jacobson et al., 1995; Love et al., 2011; Seely et al., 2003). These water resources are particularly useful for poor rural communities and small-scale agriculture as the head difference and distance from river channel to riparian fields are usually small, minimising pumping costs and infrastructure requirements, and the relatively low stored volumes are not restrictive, as they may be for water supply to a town or for large-scale irrigation (Hussey, 2007; Love et al., 2007). Consequently, sand river abstraction systems are popular with NGOs and donors, as evidenced by the number of organisations who work only on installing such systems (e.g. Dabane Trust, 2017; Excellent Development, 2017; Tarun Bharat Singh, 2017).

Understanding the frequency of flow/recharge events is crucial for planning of abstraction systems. Hence, Davies et al. (1998), state the sustainable yield of a sand river system primarily depends on “the recharge it receives and its distribution with time”. Estimation of sustainable yield means an appropriate sand river abstraction system can be designed, ranging from simple caissons and handpumps for domestic supply to banks of well points abstracting over 1000 l/s for large-scale irrigation (Clanahan and Jonck, 2004). Sand river aquifer recharge is almost entirely from surface water flow during annual/occasional floods, with direct precipitation providing minimal recharge (Owen and Dahlin, 2005; Sorman et al., 1997). Because surface water flow only occurs when the aquifer is fully saturated (Nord, 1985; Owen, 1989), surface water flow frequency equates to alluvial aquifer recharge frequency. Understanding of flow frequency is also required for a sand dam feasibility assessment according to Maddrell (2018): “Sand dams must be sited on a sufficiently seasonal river” (the number 1 technical

* Corresponding author.
E-mail address: david.walker4@newcastle.ac.uk (D. Walker).

https://doi.org/10.1016/j.jaridenv.2019.05.006
Received 29 August 2018; Received in revised form 31 March 2019; Accepted 21 May 2019
Available online 30 May 2019

pre-condition). Furthermore, because sand dams should be constructed in lifts following each surface water flow event (in order to enable passage of silts and trapping of only coarse sediment), it is important to know the flow frequency to enable project management of materials and labour (Nissen-Petersen, 2006).

Analysis of flow records would be the easiest method of determining surface flow/recharge frequency, however, such records are scarce in many regions of the world, especially in arid and semi-arid environments (Tooth, 2000). Sand river flows are often subject to downstream volume decreases, principally due to transmission losses into the riverbank and underlying geology, in addition to evaporation losses (Hughes and Sami, 1992). Therefore, unless the river has multiple gauges, surface flows in the reach under investigation may have petered out before a downstream gauge is reached and the flow/recharge event would go unrecorded. Conversely, recorded flow at an upstream gauge may have petered out before reaching the area of interest. Rainfall records could suggest flow frequency though this may be unreliable as dryland areas are characterised by high variability in rainfall amount, intensity and spatial distribution (Goudie, 1987; Koohafkan and Stewart, 2008). In more arid and larger catchments, storms may occur in a relatively isolated area, activating some tributaries and leaving adjacent tributaries dry (Tooth, 2000). The common absence of flow frequency data means that usually the only option is to identify local people with a long and deep knowledge of the sand river and simply ask them about frequency and magnitude of flow events (Neal, 2012).

Satellite remote sensing could potentially aid in estimating recharge frequency in data scarce regions through detection of surface water flow. However, the review paper by Huang et al. (2018), concerning detecting and monitoring surface water from satellite imagery, presents no previous studies assessing ephemeral channels in dryland areas. The use of remote sensing for investigating sand rivers has been mostly limited to identification and delineation of alluvial aquifers (Owen, 1989; SIDA-VIAK, 1984), even though flooding extent mapping is a well-established practice (Policelli et al., 2017; Pham et al., 2018). Mpala et al. (2016) tried using Landsat data to detect water saturated sand, but concluded that manual visual inspection of individual images would be required to determine if there was any surface flow or moisture. The narrow channel width of exploited sand rivers (a few tens of metres) and the often short duration of flow events (a few days) prevents the utilisation of low resolution satellite imagery from Landsat or MODIS. However, the higher spatial and temporal resolution of imagery from the recently launched Sentinel-2 satellites renders it applicable to sand river research. The aim of this study was to test whether high spatial resolution optical satellite imagery can be effectively used to detect flow in sand rivers and thus estimate recharge frequency of the alluvial aquifer.

2. Study sites

The two studied catchments, the Shingwidzi and the Molototsi, are both in eastern Limpopo Province, approximately 35 km apart, in northeast South Africa (Fig. 1). The climate is categorised as hot semi-arid, experiencing a single rainfall season during the summer months of November to March and high interannual variability. A distinct rainfall gradient is observed between both catchments' hilly headwaters in the west and the drier lowveld to the east. Severe droughts occur with unpredictable periodicity and in the past in Limpopo have caused crop failure and economic losses (Trambauer et al., 2015). The catchments overlie weathered regolith and Archaean gneisses and greenstones.

The Shingwidzi catchment rises in Vhembe District and lies mostly within the Kruger National Park, draining eastwards to join the Olifants River in Mozambique. The area of the catchment considered is that which lies above the Silwervis gauge in Kruger National Park, monitored by the South African Department for Water and Sanitation (DWS). This portion of the catchment covers 810 km^2 with a river length of approximately 90 km and channel width of 20–40 m near the gauge. The upper reaches comprise some villages and small-scale agriculture, however, Mopane-veld vegetation dominates this low relief catchment.

The Molototsi catchment is within Mopani District and drains eastwards to the Groot Letaba River, through Kruger National Park to also join the Olifants River. The catchment covers an area of 1170 km^2 and the river has a length of approximately 120 km with channel width of 50–90 m in the lower reaches. The upper reaches of the Molototsi catchment are hilly with populated valleys and forested slopes. Approximately 70 km^2 of these upper reaches lie above the Modjadji Dam, constructed in 1997 to supply potable water to the Groot Letaba municipal area (DWAF, 2010). Downstream of the dam and heading east away from the mountains the environment becomes flatter, drier and more sparsely populated, mostly comprising Mopane-veld vegetation.

3. Data

3.1. Shingwidzi ground observations

A gauged ephemeral river was required with recent records contemporary with the period of available satellite imagery. Despite South Africa being well-endowed in river gauging stations when compared to the rest of Africa (GRDC, 2017), appropriate flow data was difficult to find because ephemeral rivers are rarely gauged (Acuña et al., 2014), which is a principal reason for this remote sensing study. The DWS monitoring records are divided into basins and all dryland basins were searched for a compatible river. The Olifants Basin exemplifies the difficulties of the search: There are 98 DWS gauging stations in the Olifants Basin, though only 46 are still recording. Analysis of the 98 flow records (available online at https://www.dwa.gov.za/Hydrology) indicated that, while 22 showed some intermittence, only 7 experienced flows during fewer than 6 months per year, and only 3 of those are still recording (gauges on the Tsende, Shisha and Shingwidzi Rivers). The first two of these proved unsuitable for validation of the remote sensing flow detection methodology: The Tsende gauge is on a highly vegetated channel (i.e. there is no exposed sand river) immediately downstream of a large dam and the Shisha gauge is on a channel too narrow ($< \sim 12$ m) for current remote sensing analysis. The Shingwidzi River at Silwervis in Kruger National Park proved to be the only suitable river for analysis (Fig. 1). The gauge is located at a small sand dam within a sand channel of 20–40 m in width. While the sand dam has an influence on the flow regime, perhaps precluding passage of minor surface flow events, the channel experienced suitably ephemeral flows for its selection as a validation site. Flow data were obtained for the 2016 to 2018 hydrological years, coinciding with the imagery availability from Sentinel-2.

Corresponding rainfall data were obtained for the two raingauges within the Shingwidzi catchment; Woodlands raingauge is 2.5 km from the Silwervis river gauge and Shangoni raingauge is 30 km upstream (Fig. 1). These two raingauges are within Kruger National Park and are monitored by South Africa National Parks (SANParks) with data available online (http://dataknp.sanparks.org/sanparks/metacat). A summary of all the data for both study sites is presented in Table 1.

3.2. Molototsi ground observations

The Molototsi was selected to test the transferability of the methodology because it is ungauged, has a wide channel, and was reported to flow infrequently by the local community. The Molototsi is currently exploited for small-scale irrigation by riparian smallholder farmers; understanding flow and recharge frequency of this sand river is important for management of the increasingly abstracted water resources (Walker et al., 2018). As the Molototsi is ungauged, a local observer, who utilises the sand river aquifer daily for irrigation, recorded and photographed all surface flow events during the 2016/2017

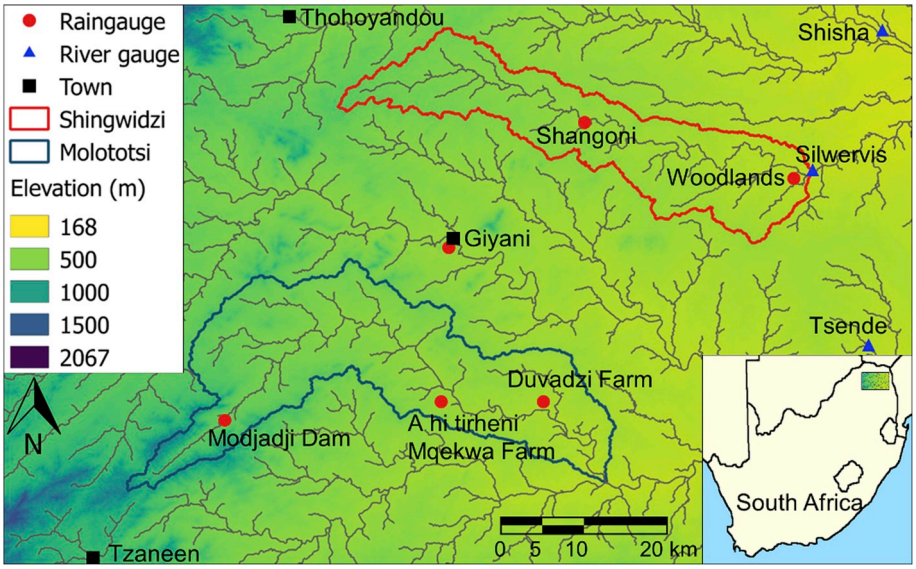

Fig. 1. Location of the study catchments, river gauges and raingauges.

hydrological year (Fig. 2). These observations of flow frequency were used to test the transferability of the remote sensing flow detection methodology.

Rainfall data were obtained for comparison with the flow records to assess if rainfall data alone could be used to predict flows in ungauged catchments. A single DWS raingauge is located within the Molototsi catchment at Modjadji Dam, its records being representative of the mountainous portion of that catchment. Two community-monitored raingauges are also present within the lowveld portion of the Molototsi catchment at A hi tirheni Mqekwa Farm and Duvadzi Farm (Fig. 1). Further rainfall measurements for the lowveld were acquired from the South African Agricultural Research Council (ARC) for their Giyani raingauge 11 km to the northeast of the catchment.

3.3. Satellite data and data pre-processing

For this study Sentinel-2 imagery was used, which offers superior spatial resolution when compared to other freely available satellite multispectral imagery (e.g. MODIS - 250 m or LandSAT - 30 m). The Sentinel-2A and -2 B satellites were developed by the European Space Agency (ESA) and were launched on 23 June 2015 and 7 March 2017, respectively. The satellites carry a multispectral instrument measuring the reflected solar spectral radiances in 13 spectral bands within the visible to the shortwave infrared (SWIR) region at three spatial resolutions (10, 20 and 60 m) and provide a 5-day revisit time.

The calibrated top-of-atmosphere (TOA) reflectance data, termed Level 1C products, with varying cloud cover (from 0 up to 61.2%) were acquired for the study areas for the 2016–2018 (Shingwidzi) and 2016/2017 (Molototsi) hydrological years. These were atmospherically corrected to bottom-of-atmosphere (BOA) reflectance products, termed Level 2 A, using Sen2Cor (version 2.4.0) with default parameter settings (Fig. 3). Sen2Cor is a third-party plugin supported by ESA for the Sentinel-2 toolbox, which performs atmospheric correction with DDV (Dark Dense Vegetation) algorithm (Kaufman et al., 1997), cloud screening and basic scene classification of Level 1C input data.

4. Methodology

The spectral regions, which are universally used in surface water and flooding monitoring studies, include the red, near infrared and shortwave infrared wavelengths. Common spectral indices utilising those regions that are used for delineation of open water features include Normalised Difference Vegetation Index (NDVI) (Tucker, 1979), Normalised Difference Water Index (NDWI) (McFeeters, 1996), Modified Normalised Difference Water Index (MNDWI) (Xu, 2006) and Normalised Difference Pond Index (NDPI) (Lacaux et al., 2007). MNDWI and NDPI utilise the shortwave infrared region, which provides greater contrast between water and non-water features when compared to near infrared wavelengths. However, the use of those indices would restrict the spatial resolution to 20 m. To take advantage of the available 10 m spatial resolution, the analysis focused on retrieval and analysis of NDWI, which was calculated using the following formula:

$$NDWI_i = (GREEN - NIR)/(GREEN + NIR)$$

Where $NDWI_i$ is NDWI value for a given day (i), GREEN is the green spectral band (band 3) and NIR is the near infrared spectral band (band 8). Water features are enhanced by NDWI and would result in positive values, whilst vegetation and soil features would usually have zero or negative values. However, such threshold would be ineffective for detecting water features within the investigated sand river. The NDWI value of the riverbed remained negative in most cases during the wet season due to the water features being very shallow and rich in sediments, which affects the absorption and scattering of light energy. Selection of an alternative threshold could be attempted, but might

Table 1
Summary of data used in the study. See Fig. 1 for ground observation locations.

Type	Location	Period	Source
River flow	Shingwidzi River @ Silwervis	Oct 16 to Jan 18	DWS
Rainfall	Woodlands and Shangoni	Oct 16 to Jan 18	SANParks
Sentinel-2 1C products	Shingwidzi watershed	Oct 16 to Jan 18	Copernicus Open Access Hub
Flow occurrence	Molototsi River, Duvadzi Farm	Oct 16 to Sep 17	Local observer
Rainfall	Modjadji Dam, Giyani, A hi tirheni Mqekwa Farm and Duvadzi Farm	Oct 16 to Sep 17	DWS, ARC, local observers
Sentinel-2 1C products	Molototsi watershed	Oct 16 to Sep 17	Copernicus Open Access Hub

Fig. 2. Examples of local observer's photographs of flow in the Molototsi River: bank-full flow on 29 December 2016 (left) and receding flow on 17 January 2017.

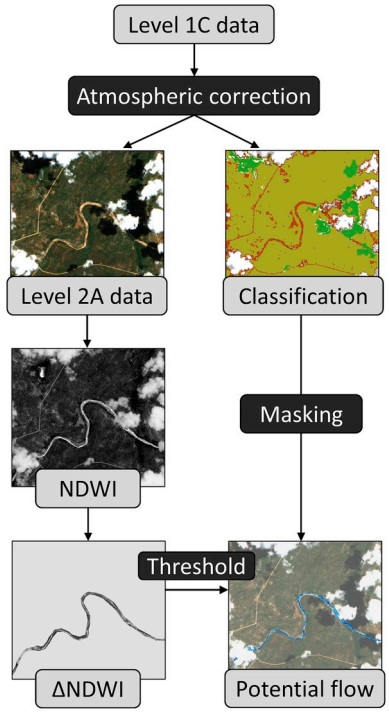

Fig. 3. The flow chart shows the implemented processing steps: (1) atmospheric correction of Level 1C data, which outputs Level 2 A data and a land-cover classification map, (2) calculation of Normalised Difference Water Index (NDWI), (3) calculation of change in NDWI relative to dry season's NDWI value (ΔNDWI), (4) implementation of a threshold, and (5) masking of areas obstructed by clouds or cloud shadows.

prove unfeasible since the spectral response throughout the river channel is variable even during the dry season. Instead, we proposed to make a pixel-level comparison of the retrieved NDWI values against dry season NDWI values, which were retrieved from imagery dated 17 July 2017 for Shingwidzi and 6 July 2017 for Molototsi. The particular dates were selected as they are at the peak of the dry season and cloud-free imagery was available. Changes between the current and the dry season's NDWI values (termed $NDWI_{dry}$) within the river channel were expressed as a percent difference on a per-pixel basis:

$$\Delta NDWI_i = (NDWI_{dry} - NDWI_i)/ NDWI_{dry} \times 100$$

Calculation of ΔNDWI was restricted to river channels. The value of the threshold signifying flow was selected upon investigation of the ΔNDWI variability on another cloud-free image acquired during the dry season: 17 August 2017 for Shingwidzi and 10 August 2017 for Molototsi. River polylines, digitised manually along the whole length of the river channels' centres, were used to extract ΔNDWI values along the riverbeds. All pixels within a 5 m buffer of the polylines, i.e. one pixel width, were used for analysis. This ensured all pixels utilised for calculation of the threshold comprised only sand river channel and excluded all mixed pixels. The mean ΔNDWI and standard deviation values were 3.11% and 11.93% for the Shingwidzi river channel, 7.59% and 6.73% for the Molototsi river channel. The variation within each channel could be attributed to such factors as change in the sand properties leading to a change in reflectance or the performance of the applied atmospheric correction. Early validation results for a site in Germany of the used Sen2Cor processor showed a difference of up to 4% between image and reference reflectance values leading to an NDVI uncertainty of up to 6% (Pflug et al., 2016). The uncertainty of NDWI retrieved in this study could be higher as challenging imagery with very high cloud cover (up to 61.2%) were used to achieve the highest possible temporal resolution. We aimed to account for 95% of variation within the ΔNDWI value, which would require a threshold of 20.82% for Shingwidzi and 20.04% for Molototsi (based on the 95th percentile); these values were rounded to 21% and 20%, respectively, for the analysis. Where ΔNDWI surpassed the chosen threshold, the pixel was classified as likely to contain surface water. Areas identified as clouds or cloud shadows were masked using the 20 m classification product derived by the Sen2Cor processor.

Presence of flow was determined based on analysis of threshold outputs; whenever highlighted pixels formed linear patterns within the river channel, a flow was recorded. Confusion matrices comparing ground observations to satellite predictions were used to assess the performance of the methodology. The number of true positives (TP) representing correctly detected flows, true negatives (TN) representing correct identification of no flow, false positives (FP) representing incorrectly detected flows and false negatives (FN) representing undetected flows were used to derive four statistical measures (Mann and Lacke, 2010), where n is the total number of analysed satellite passes:

- Overall accuracy: How often was the prediction correct? (TP + TN)/n
- Recall, or true positive rate: How often was a flow correctly identified? TP/(TP + FN)
- Precision: How often did flow occur when flow was predicted? TP/(TP + FP)
- f1-score: A measure of the methodologies accuracy; defined as the harmonic mean of recall and precision. 2TP/(2 TP + FP + FN).

5. Results and discussion

5.1. Validation of methodology at shingwidzi

It can be seen in Fig. 4 that surface flows are detectable from Sentinel-2 imagery; high flows are observable in January with lower flows in November and February. The quantitative validation of flows identified with Sentinel-2 versus formally observed flows in the Shingwidzi River show that the methodology performs very well. The confusion matrices and associated accuracy statistics are shown in Table 2 and reveal high overall accuracy, recall and f1-score, while precision is lower.

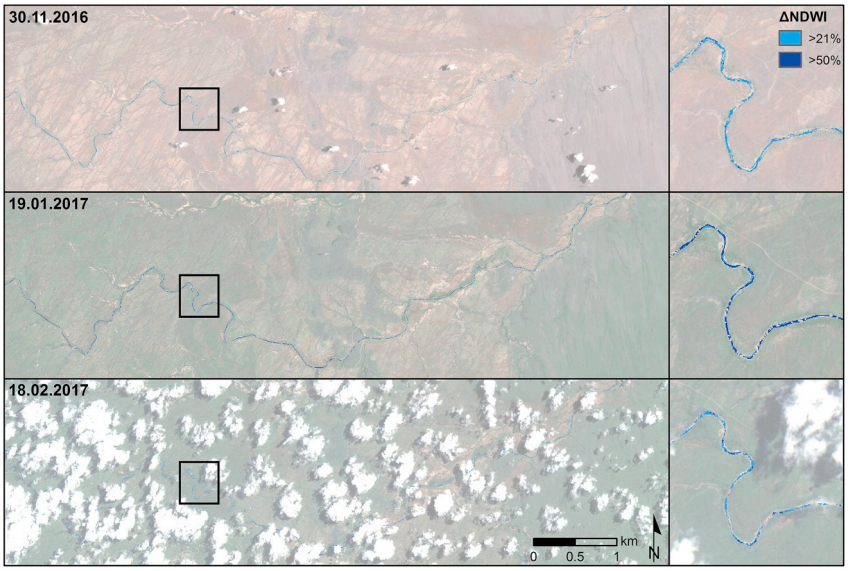

Fig. 4. Examples of processed imagery for the Shingwidzi River showing flow. The box shows the location of the magnified image on the right.

The high scores result from the fact there was only a single false negative (undetected flow). This single false negative occurred when substantial cloud cover permitted analysis of only short sections of the river and at the end of a multi-week flow event when receding flow was very low. However, previous satellite passes did detect the flow (see Fig. 5). From a point of view of detecting aquifer recharge events, it is most important the flow was detected at all rather than informing its duration. More concerning are the five false positives (incorrectly detected flows). Further investigation revealed that these five false positives were caused by misregistration of imagery resulting from differences in image geometry. The latest multi-temporal image registration performance report indicates the imagery are registered to within 11 m (for Sentinel-2A) and 13 m (for Sentinel-2B) at 95% confidence level. The statistics have shown that 60% of Sentinel-2A and 42% of Sentinel-2B products have co-registration error of less than 0.5 pixels, whilst error of less than one pixel was observed for 92% of Sentinel-2A and 86% of Sentinel-2B products (ESA, 2018). Because the Shingwidzi channel is generally only two to four pixels (20–40 m) wide, geometric offset of a few metres was sufficient to give ΔNDWI values above the threshold as bankside vegetation was now incorporated into sand river pixels. Geometric correction could have been conducted manually but this is not a practical option for multi-temporal image analysis. In this respect, conventional threshold methods may appear to be better performing as they are independent of image misregistration. However, in the investigated rivers, reflectance varied throughout the sand river channel, even during the dry season, rendering this conventional threshold method unfeasible. ESA is currently developing a further geometric refinement algorithm to improve the repetitiveness of the image geolocation and eventually reach the multi-temporal geolocation requirement of the mission (< 0.3 pixel at 95% confidence level) (ESA, 2018; Yan et al., 2018), which should minimise this problem. It will be seen in the subsequent section that this issue did not occur with the Molototsi. This is due to the Molototsi channel being 50–90 m wide, therefore, with geometric offset of a few metres most sand river pixels would remain largely unaffected. Three conclusions could be drawn: 1) The minimum sand river channel width to negate false negatives induced by image misregistration is about 40 m, so that at least two pixels would only be minimally affected. 2) Only Sentinel-2 (excluding commercial providers) with its 10 m resolution is suitable for sand river analysis; geometric offset of coarser resolution satellite imagery would restrict the analysis to very large sand rivers. 3) The methodology generally performed satisfactorily and could be tested at the Molototsi.

5.2. Transferability of methodology at molototsi

Quantitative validation of the Molototsi was conducted as per the Shingwidzi. Flow events observed and photographed were compared to predicted flows (Table 3)..

The accuracy statistics for the Molototsi are very high, better than for the Shingwidzi, due to image misregistration not being an issue in

Table 2
Confusion matrix and accuracy assessment of flow and no flow detection in the Shingwidzi River for the period 1/10/2016 to 31/1/2018 (the most recent available data). The values within the matrix refer to observations or predictions of satellite passes as opposed to days of flow or number of events. Satellite passes when cloud cover prevented analysis are not included in the matrix and are discussed later in the manuscript. For the temporal distribution of the cloud obscured passes, see Fig. 5.

n = 68	Observed flow	Observed no flow
Predicted flow	10	5
Predicted no flow	1	52

Overall accuracy (%):	91.2
Recall (%):	90.9
Precision (%):	66.7
F1-score:	0.77
No. Of satellite passes obscured by cloud:	66/134 (49.3%)

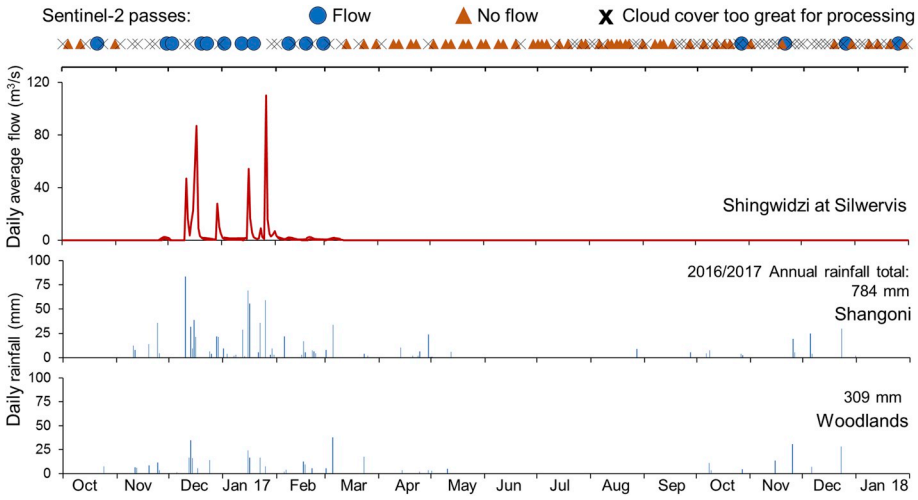

Fig. 5. All Sentinel-2 passes during the 2016/2018 hydrological years – to the limit of river flow data availability in February 2018 – showing whether or not surface water flow was detected in the Shingwidzi River and when cloud cover was too extensive for processing (top); the river hydrograph measured at the Silwervis gauge, and; local rainfall records showing the 2016/2017 annual total for comparison between raingauges. It should be noted that 2016/2017 was above average for rainfall and flows. The increased frequency of satellite passes in July 2017 reflects the onset of data availability from the second Sentinel-2 satellite.

the wider sand channel and thus not producing false positives. However, there was a flow event in May that was undetected by Sentinel-2 (see Fig. 6). This event being undetected resulted not from an error but from the lack of a satellite pass during a very short duration flow. This flow event was observed by the authors (Fig. 7) and occurred a few hours after a 12th May satellite pass. The flow had completely receded giving way to a dry sand surface prior to the subsequent satellite pass on 19th May. This flow event occurred in May 2017 prior to data availability from both Sentinel-2 satellites. As the frequency of images is now every 2–5 days, it is not expected that such a short-lived flow would be subsequently undetected (unless obscured by cloud cover). This event confirms that currently only Sentinel-2 with its high temporal resolution is applicable to sand river flow detection. This ground observation revealed that detecting bank-full flows would be unlikely as they may occur for just a few hours (Fig. 7b). Therefore, unless the satellite is extremely fortuitously overflying during that brief period and cloud cover is not extensive, identification of flow requires detecting receding flow when only a narrow stream exists within the channel (Fig. 7c). The spatial resolution of Sentinel-2 imagery was sufficiently high for these receding flows to be detected, as is shown in Fig. 8. What's more, disconnected (at least on the surface) pools remained visible on the imagery in the days following flow cessation (Fig. 8). This indicated surface flow occurred recently even when that flow may have been missed due to cloud cover or no satellite pass. It can be seen qualitatively in Fig. 8 that surface flows can be identified with NDWI from Sentinel-2. An active flowing stream is clearly visible within the moist sand river channel. The sand river can then be observed to become progressively drier until baseline conditions are resumed after about a month.

5.3. Sources of uncertainty

In addition to the previously discussed issue of image misregistration, which can be negated by applying the methodology in suitably wide rivers, sources of uncertainty include the accuracy of the river channel polyline and cloud cover. Inaccurate digitisation of river polylines may result in incorporation of mixed pixels leading to errors in the ΔNDWI threshold. Determination of this threshold from the whole river channel rather than the channel centre may provide a more representative value but similarly there is the risk of incorporating mixed pixels. The issue of short-lived flows occurring between Sentinel-2 satellite passes is now considered unlikely due to the increased temporal resolution since the launch of Sentinel-2B.

The main limitation of using optical remote sensing instruments, and consequently of the presented methodology, is their vulnerability to cloud cover. Tables 2 and 3 show that 49.3% and 36.9% of the Shingwidzi and Molototsi images, respectively, could not be processed due to excessive cloud cover. The poorer percentage of processable images for the Shingwidzi was because a relatively short length of the sand river (20 km) at the flow gauge was analysed; the downstream reach being prior to any significant tributaries which may contribute flows that did not pass the flow gauge. In the case of the Molototsi, a longer reach was analysed (approximately 90 km) giving more chance of detecting flow within breaks in cloud cover. Since the launch of the second Sentinel-2 satellite, a single non-processable image may not be an issue as if flow goes undetected the surface water would likely remain until the subsequent overflight. However, where multiple consecutive images cannot be processed, and pre-July 2017 when the period between image acquisitions was greater, there exists the

Table 3
Confusion matrix and accuracy assessment of flow and no flow detection in the Molototsi River for the period 1/10/2016 to 30/9/2017. The values within the matrix refer to observations or predictions of satellite passes as opposed to days of flow or number of events. Satellite passes when cloud cover prevented analysis are not included in the matrix and are discussed later in the manuscript. For the temporal distribution of the cloud obscured passes, see Fig. 6.

n = 53	Observed flow	Observed no flow
Predicted flow	7	0
Predicted no flow	0	46

Overall accuracy (%):	100
Recall (%):	100
Precision (%):	100
F1-score:	1.00
No. Of satellite passes obscured by cloud:	31/84 (36.9%)

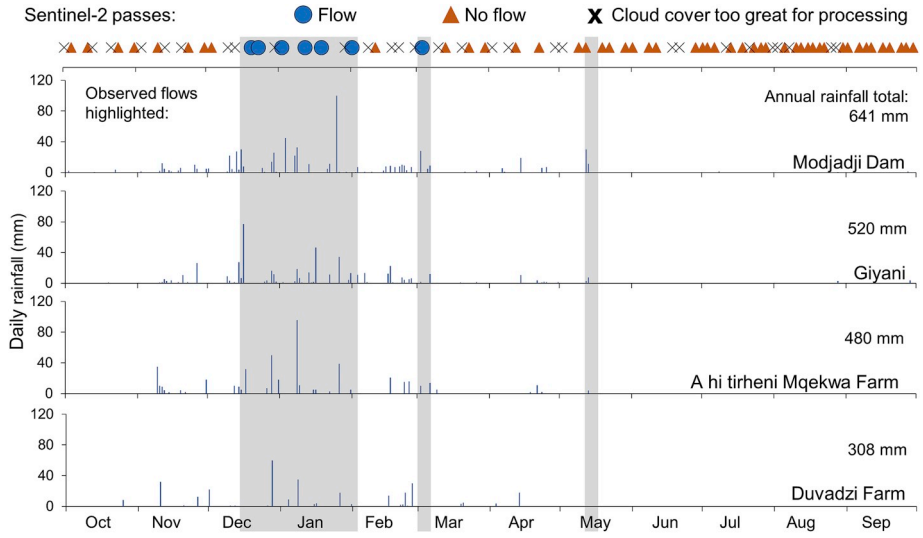

Fig. 6. All Sentinel-2 passes during the 2016/2017 hydrological year showing whether or not surface water flow was detected in the Molototsi River and when cloud cover was too extensive for processing (top); local rainfall records, and; local observer's ground observations of flow events highlighted in grey.

Fig. 7. The Molototsi River when dry at 09:24 on 12 May 2017 (a), during short-lived bank-full flow at 12:50 on 13 May (b), and receding flow at 15:22 on 13 May (c).

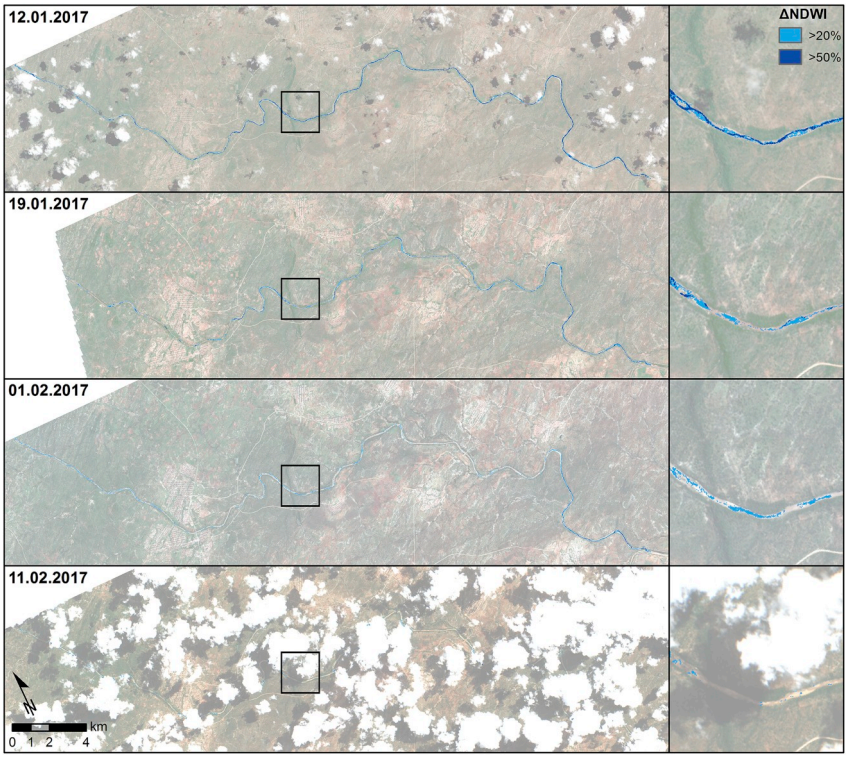

Fig. 8. Examples of processed imagery for the Molototsi River showing significant flow (12 January), receding flow (19 January), disconnected pools (1 February), and no surface water (11 February). The box shows the location of the magnified image on the right.

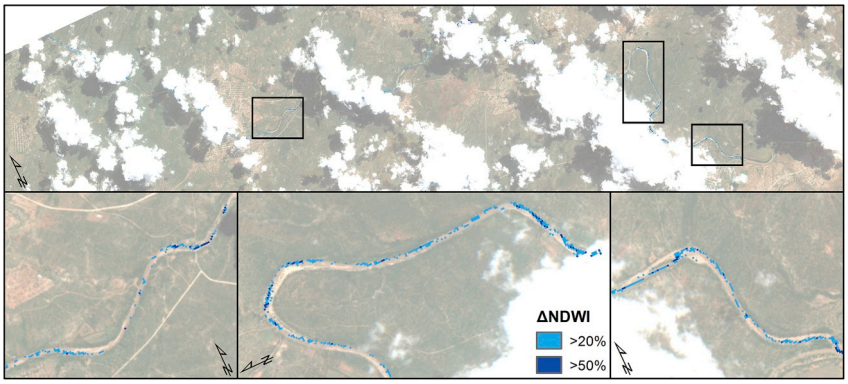

Fig. 9. Processing output for 3 March 2017 with magnified locations used for visual analysis to determine the presence of flow in the Molototsi River.

possibility of not detecting flows. Furthermore, care has to be taken if imagery with a significant cloud cover is used for the analysis as the Sen2Cor processor may not always produce an optimal classification result. If some pixels occupied by clouds or their shadow are not classified as such, they will not be masked from the final result, and consequently may be misidentified as flow. Fig. 8 shows such an example for the imagery acquired on 11 February 2017; several isolated pixel clusters are highlighted as potential flow due to the classification failing to identify they are located within the cloud shadow. An alternative algorithm, such as the one developed by Zhu et al. (2015), could be used to improve the cloud detection accuracy, although that would require implementation of a further processing step. We therefore recommend comparing the processing outputs against the original image if disconnected pools are identified within a very cloudy scene to ensure they are not located within a cloud or a shadow. Despite this limitation, in this study image tiles with cloud cover as high as 61.2% were successfully processed and analysed. Fig. 9 shows how flow can still be identified even when the river is partially obstructed by clouds; inspection of the visible sections of the river suggested a receding flow was present on that day.

5.4. Comparison with rainfall and nearby flow records

Flow within the studied sand rivers was compared to raingauge records to assess whether satellite imagery is necessary to detect surface flow events or could rainfall data more easily predict flow in ungauged catchments. While Figs. 5 and 6 show that flows occurred during the period of highest rainfall, there are individual high rainfall totals that did not cause flows and flows when rainfall was not especially high. It appears that rainfall, therefore, is a poor predictor of surface flow events. This is due to the high spatial variability of rainfall indicating that the rainfall monitoring network would have to be of very high density to be sufficient to identify if and/or when flows occurred. The May 2017 flow event (Fig. 7) was revealing in that the raingauges within the lowveld (at Giyani, A hi Tirheni Mqekwa Farm and Duvadzi Farm) recorded little rainfall (0–10.3 mm), though 41.5 mm was measured at Modjadji Dam (Fig. 6). What's more, no flow was observed in the Molototsi tributaries in the lowveld; the only tributaries observed to be active were those from the small proportion of the mountain catchment downstream of Modjadji Dam. Visits to farms near Giyani on the adjacent Klein Letaba River (between the Molototsi and Shingwidzi catchments) showed that this river had not experienced flood flows, and the Shingwidzi flow data show no flow occurred there either (Fig. 5). This short duration flow event provided complete recharge to the Molototsi sand river aquifer though could not be predicted from nearby raingauge nor river flow records.

6. Conclusions

This research has shown that remote sensing can aid in estimating sand river flow and recharge frequency, and enhance ground-based monitoring networks. The presented methodology of analysing change in NDWI value calculated using Sentinel-2 imagery successfully detected surface flows, even when flow had substantially receded and during substantial cloud coverage. A disadvantage of the method, akin to all applications of optical remote sensing, is its dependence on limited cloud cover. However, we showed that by investigating a lengthy reach of a river, the proportion of non-processable imagery can be substantially reduced. The methodology proved applicable and successful on two South African sand rivers and should be transferrable to other sand rivers around the world. The only site-specific element is the calculation of the ΔNDWI threshold that has some dependence on the dry season reference value. The 10 m spatial resolution means sand rivers as narrow as 20 m are theoretically analysable as long as the imagery contains pixels comprising only sand river. However, as was revealed by the study, problems of geometric correction mean 40 m is proposed as the minimum sand river width to avoid tedious manual registration of individual images. The minimum analysable channel width will further depend on riparian vegetation overhang.

Use of remote sensing allows investigation of the potential for a sand river to provide an exploitable water resource, whilst minimising field costs and risks, including avoidance of in-situ instrumentation and associated risks of vandalism or theft. The potential applications of this methodology include:

- Estimation of recharge frequency in sand rivers where no flow gauges, raingauges or anecdotal records exist, to enhance ground-based monitoring networks
- Estimation of recharge frequency in sand rivers that may be too costly or too hazardous to visit
- Estimation of recharge frequency, which, when combined with field aquifer geometry measurements, can be used to determine sustainable yield
- Exclusion from further investigation at desk study stage of unsuitable sand rivers that receive infrequent surface flows
- Extraction of information that enables planning, particularly timing, of sand abstraction system construction
- Corroboration of anecdotal evidence of surface flow frequency
- Determination of preceding rainfall thresholds (if headwater rainfall records are available) that cause surface flows and recharge from specific runoff source areas
- Determination of preceding upstream flow or dam release thresholds (if upstream gauge or dam release records are available) that cause surface flows and recharge

Acknowledgements

David Walker was funded under the SAgE Faculty (Newcastle University Faculty of Science, Agriculture and Engineering) DTA programme. Fieldwork was supported by the John Day Bursary from the International Association of Hydrogeologists. The authors acknowledge the Water Research Commission for funding project No. K5/2426, the Limpopo Department of Agriculture and Rural Development for in-kind contributions, the local observer for monitoring rainfall and river flow, and the Institute for Soil, Climate and Water (Agricultural Research Council), SANParks and Department of Water and Sanitation (DWS) for providing weather data.

References

Acuña, V., Datry, T., Marshall, J., Barceló, D., Dahm, C.N., Ginebreda, A., McGregor, G., Sabater, S., Tockner, K., Palmer, M.A., 2014. Why should we care about temporary waterways? Science 343 (6175), 1080–1081.

Clanahan, M., Jonck, J.L., 2004. A Critical Evaluation of Sand Abstraction Systems in Southern Africa. Report to the Water Research Commission on the Project "Systems for the Abstraction of Wa Ter through River Sand Beds". WRC, Pretoria, South Africa.

Dabane Trust, 2017. http://www.dabane.co.zw, Accessed date: 19 November 2017.

Davies, J., Rastall, P., Herbert, R., 1998. Final Report on Application of Collector Well Systems to Sand Rivers Pilot Project. British Geological Survey, Wallingford, UK BGS Report WD/98/2C.

DWAF, 2010. Review of Water Requirements, vol. 2 Department of Water Affairs, South Africa.

ESA, 2018. Sentinel-2 L1C Data Quality Report Issue 28 Ref. S2-PDGS-MPC-DQR. (04/08/2018). [Online]. https://earth.esa.int/web/sentinel/user-guides/sentinel-2-msi/document-library, Accessed date: 25 August 2018.

Excellent Development, 2017. http://www.excellentdevelopment.com, Accessed date: 19 November 2017.

Goudie, A.S., 1987. Change and Instability in the Desert Environment, Horizons in Physical Geography. Springer, pp. 250–267.

GRDC, 2017. Global Runoff Data Centre, a Repository for the World's River Discharge Data and Associated Metadata. http://www.bafg.de/GRDC, Accessed date: 2 December 2017.

Huang, C., Chen, Y., Zhang, S., Wu, J., 2018. Detecting, extracting, and monitoring surface water from space using optical sensors: a review. Rev. Geophys. 56 (2), 333–360.

Hughes, D.A., Sami, K., 1992. Transmission losses to alluvium and associated moisture dynamics in a semiarid ephemeral channel system in southern Africa. Hydrol. Process. 6 (1), 45–53.

Hussey, S.W., 2007. Water from Sand Rivers. Guidelines for Abstraction. Water, Engineering and Development Centre (WEDC). Loughborough University of Technology, UK 194pp.

Jacobson, P.J., Jacobson, K.N., Seely, M.K., 1995. Ephemeral Rivers and Their Catchments: Sustaining People and Development in Western Namibia. Desert Research Foundation of Namibia, Windhoek, Namibia 164pp.

Kaufman, Y.J., Wald, A.E., Remer, L.A., Bo-Cai, G., Rong-Rong, L., Flynn, L., 1997. The MODIS 2.1-μm channel-correlation with visible reflectance for use in remote sensing of aerosol. IEEE Trans. Geosci. Remote Sens. 35 (5), 1286–1298. https://doi.org/10.1109/36.628795.

Koohafkan, P., Stewart, B.A., 2008. Water and Cereals in Drylands. Food and Agriculture Organisation. (FAO) of the United Nations and Earthscan, London, UK, pp. 113.

Lacaux, J.P., Tourre, Y.M., Vignolles, C., Ndione, J.A., Lafaye, M., 2007. Classification of ponds from high-spatial resolution remote sensing: application to Rift Valley Fever epidemics in Senegal. Rem. Sens. Environ. 106 (1), 66–74. https://doi.org/10.1016/j.rse.2006.07.012.

Love, D., Hamer, W.d., Owen, R., Booij, M., Uhlenbrook, S., Hoekstra, A., Zaag, P., 2007. Case studies of groundwater: surface water interactions and scale relationships in small alluvial aquifers. In: 8th WATERNET/WARFSA/GWP-SA Symposium, 31 October - 2 November 2007, pp. 6 Lusaka, Zambia.

Love, D., van der Zaag, P., Uhlenbrook, S., Owen, R.J.S., 2011. A water balance modelling approach to optimising the use of water resources in ephemeral sand rivers. River Res. Appl. 27 (7), 908–925.

Maddrell, S.R., 2018. Sand Dams: A Practical & Technical Manual. Excellent Development. http://www.excellectdevelopment.com, Accessed date: 20 July 2018.

Mann, P.S., Lacke, C.J., 2010. Introductory Statistics. John Wiley & Sons Canada Ltd, Mississauga, Canada.

McFeeters, S.K., 1996. The use of the normalized difference water index (NDWI) in the delineation of open water features. Int. J. Remote Sens. 17 (7), 1425–1432. https://doi.org/10.1080/01431169608948714.

Mpala, S.C., Gagnon, A.S., Mansell, M.G., Hussey, S.W., 2016. The hydrology of sand rivers in Zimbabwe and the use of remote sensing to assess their level of saturation. Phys. Chem. Earth 93, 24–36. https://doi.org/10.1016/j.pce.2016.03.004.

Neal, I., 2012. The potential of sand dam road crossings. Dams Reservoirs 22 (3–4), 129–143.

Nissen-Petersen, E., 2006. Water from Dry Riverbeds. ASAL Consultants Limited for the Danish International Development Agency (DANIDA), Nairobi, Kenya, pp. 68pp.

Nord, M., 1985. Sand Rivers of Botswana, Results from Phase 2 of the Sand Rivers Project. Department of Water Affairs, Government of Botswana, Gaborone Unpublished report.

Owen, R., Dahlin, T., 2005. Alluvial aquifers at geological boundaries: geophysical investigations and groundwater resources. Groundwater and Human Development: IAH Selected Papers on Hydrogeology 6, 233.

Owen, R.J.S., 1989. The Use of Shallow Alluvial Aquifers for Small Scale Irrigation with Reference to Zimbabwe. University of Zimbabwe and Southampton University, UK, pp. 121 Final report of ODA Project R4239.

Pflug, B., Main-Knorn, M., Bieniarz, J., Debaecker, V., Louis, J., 2016. Early validation of sentinel-2 L2A processor and products. In: Ouwehand, L. (Ed.), Living Planet Symposium 2016, pp. 1–6 Prague, Czech Republic.

Pham, H.T., Marshall, L., Johnson, F., Sharma, A., 2018. Deriving daily water levels from satellite altimetry and land surface temperature for sparsely gauged catchments: a case study for the Mekong River. Rem. Sens. Environ. 212, 31–46.

Policelli, F., et al., 2017. The NASA global flood mapping system. In: Lakshmi, V. (Ed.), Remote Sensing of Hydrological Extremes. Springer International Publishing, pp. 47–63. https://doi.org/10.1007/978-3-319-43744-6_3.

Seely, M., et al., 2003. Ephemeral and Endoreic River Systems: Relevance and Management Challenges. Transboundary Rivers, Sovereignty and Development: Hydropolitical Drivers in the Okavango River Basin. pp. 187–212.

SIDA-VIAK, 1984. Remote Sensing for Water Resources Development, Provisional Military Government of Socialist Ethiopia. Cited in: Owen, R.J.S. 1989. The Use of Shallow Alluvial Aquifers for Small Scale Irrigation with Reference to Zimbabwe. Final Report of ODA Project R4329. University of Zimbabwe and Southampton University, UK.

Sorman, A.U., Abdulrazzak, M.J., Morel-Seytoux, H.J., 1997. Groundwater recharge estimation from ephemeral streams. Case study: wadi Tabalah, Saudi Arabia. Hydrol. Process. 11 (12), 1607–1619.

Tarun Bharat Singh, 2017. http://tarunbharatsangh.in/, Accessed date: 19 November 2017.

Tooth, S., 2000. Process, form and change in dryland rivers: a review of recent research. Earth Sci. Rev. 51 (1), 67–107.

Trambauer, P., et al., 2015. Hydrological drought forecasting and skill assessment for the Limpopo River basin, southern Africa. Hydrol. Earth Syst. Sci. 19 (4), 1695–1711.

Tucker, C.J., 1979. Red and photographic infrared linear combinations for monitoring vegetation. Rem. Sens. Environ. 8 (2), 127–150. https://doi.org/10.1016/0034-4257(79)90013-0.

UN, 2017. United Nations 2010-2020 Decade for Deserts and the Fight against Desertification. http://www.un.org/en/events/desertification_decade/, Accessed date: 19 November 2017.

Walker, D., Jovanovic, N., Bugan, R., Abiye, T., du Preez, D., Parkin, G., Gowing, J., 2018. Alluvial aquifer characterisation and resource assessment of the Molototsi sand river, Limpopo, South Africa'. J. Hydrol.: Reg. Stud. 19, 177–192.

Xu, H.Q., 2006. Modification of normalised difference water index (NDWI) to enhance open water features in remotely sensed imagery. Int. J. Remote Sens. 27 (14), 3025–3033. https://doi.org/10.1080/01431160600589179.

Yan, L., Roy, D., Li, Z., Zhang, H., Huang, H., 2018. Sentinel-2A multi-temporal misregistration characterization and an orbit-based sub-pixel registration methodology. Remote Sens. Environ. 215, 495–506.

Zhu, Z., Wang, S., Woodcock, C.E., 2015. Improvement and expansion of the Fmask algorithm: cloud, cloud shadow, and snow detection for Landsats 4–7, 8, and Sentinel 2 images. Rem. Sens. Environ. 159, 269–277. https://doi.org/10.1016/j.rse.2014.12.014.